

Mixture Theory Model of Vortex Sand Ripple Dynamics

A.M. Penko and J. Calantoni
Marine Geosciences Division

Introduction: Our lack of understanding of the evolution of seabed roughness (e.g., sand ripples) in sandy coastal regions inhibits our ability to accurately forecast waves and currents and ultimately large-scale morphodynamics. Most wave and circulation models input a constant bottom roughness value (i.e., friction factor) or fixed bed profile that parameterizes the effects of seabed roughness, ignoring any temporal or spatial response of the bed to changing wave and sediment conditions. However, seabed roughness length scales may span three orders of magnitude (e.g., from grain-scale variations to sand ripples), causing significant differences in boundary layer turbulence, wave energy dissipation, coastal circulation, and sediment transport. The constant evolution of the seabed also has significant implications for naval operations (e.g., ocean acoustics, mine hunting missions, littoral navigation).

All bathymetric change ultimately results from sediment entrainment and deposition occurring at the fluid-sediment interface inside the wave bottom boundary layer (WBBL). Despite the apparent accessibility of the phenomena, highly turbulent, sediment-laden flow remains poorly understood and difficult to quantify mainly because of our failure to understand the fundamental interaction forces driving sediment transport. However, with recent advances in high performance computing, it is now possible to perform highly resolved simulations of fluid-sediment dynamics in the WBBL that accurately model the evolution of seabed roughness for sandy substrates. The high-resolution model described here (SedMix3D) is based on mixture theory. Although the approach is well known and understood for industrial and biological applications, it has never before been applied to coastal sediment dynamics.

Mixture Theory Model: Mixture theory treats a fluid-sediment mixture as a single continuum with effective properties that parameterize the fluid-sediment and sediment-sediment interactions (e.g., hindered settling, particle pressure, and diffusion). SedMix3D predicts the time-dependent sediment concentration and three-component velocity field under varying wave conditions. The bulk mixture parameters (e.g., density and viscosity) are dependent on the local sediment concentration of the fluid-sediment mixture. Grid spacing is on the order of a sediment diameter and time steps are nearly four orders of magnitude less

than the smallest turbulent fluid temporal scale. Using the Message-Passing Interface (MPI) for parallelization, SedMix3D may be run on up to 512 processors on high performance computing (HPC) architectures. The development and optimization of SedMix3D and the analysis presented here have utilized over 1.5 million CPU hours and over 5 TB of storage space provided by the DoD High Performance Computing and Modernization Program during the past two years.

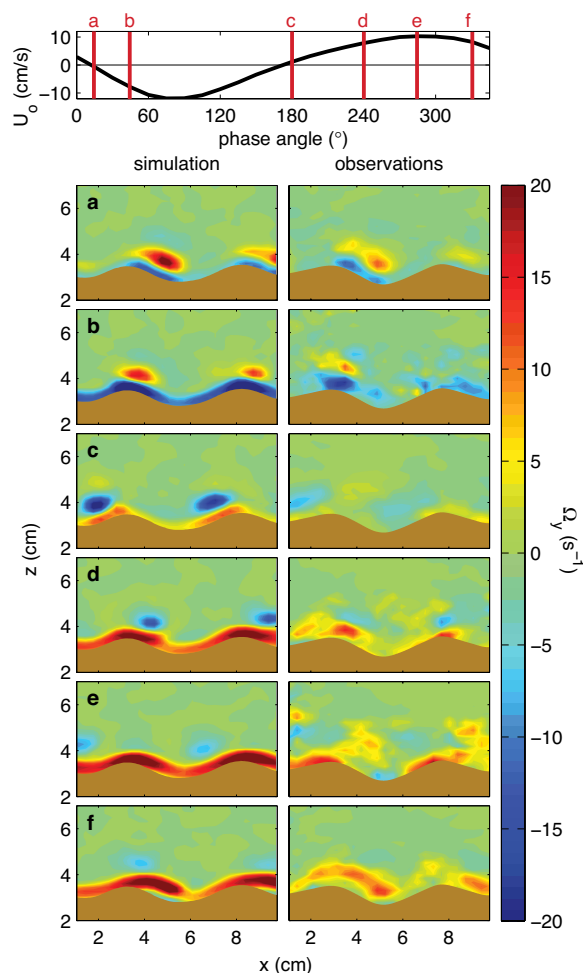


FIGURE 1

Ensemble-averaged model and observed vorticity fields, Ω_y (s^{-1}), at six phase locations of a wave are plotted in the contoured panels. The top graphic is a plot of the ensemble-averaged free stream wave velocity where the red lines indicate phase location of panels a through f. Flow is initially directed to the left (onshore). Positive (red) contours in panels a through f indicate clockwise rotation. A time-average of the simulated (left) and observed (right) bed profile is contoured in brown for reference. The model predicts the location, size, and rotational direction of the vortices for all phases shown. The shape of the vortex structure, including the vortex tails (the area of vorticity connecting the ejected vortex to the generation point, as in panels a and f) predicted by the model is also in good agreement with the observations.

Model Validation: Simulated vorticity fields, swirling strength, and mean horizontal and vertical velocities were recently compared to particle image velocimetry (PIV) data obtained from a free surface laboratory flume. Comparisons of time-varying vorticity and bulk flow statistics to laboratory measurements show the model in excellent agreement with observations. The modeled and observed ensemble-averaged vorticity fields are plotted in Fig. 1. The results of the comparisons show that SedMix3D does provide an accurate representation of turbulent flow over ripples for the conditions represented by the experiments. Additionally, SedMix3D has been found to predict sand ripple geometries (i.e., ripple height and wavelength) under a range of flow conditions typically found in the laboratory and also simulates the transition from one ripple state to another.¹ SedMix3D is a powerful research tool that may now be used to better understand the currently unknown effects of sand ripples.

Research Applications: SedMix3D provides details of small-scale sand ripple dynamics and may be used to understand presently unknown phenomena including (1) the effects of suspended sediment concentration on turbulence modulation, (2) the dynamics of ripple transitions from 2D to 3D (and back to 2D) under changing forcing conditions, and (3) the role of terminations and bifurcations on ripple migration and growth rates. These processes are important in determining the quantity of wave energy dissipated by seabed roughness. SedMix3D allows for the quantification of the effects of seabed morphology on the generation and dissipation of boundary layer turbulence. Recently, simulations of flow over a bifurcated ripple (two parallel ripples connected by a diagonal ripple between them) produced a substantial increase in the production of boundary layer turbulence when compared to the same simulation without the bifurcation. The excess turbulence significantly increased the boundary layer thickness (Fig. 2).

Summary: Ultimately, all process-based models for nearshore bathymetric evolution are limited by shortcomings in fundamental knowledge of multiphase boundary layer physics. SedMix3D provides an unprecedented level of detail for the study of fluid-sediment interactions that is impossible to obtain with available measuring technologies in the field or laboratory. Our current lack of detailed knowledge of vorticity dynamics and the transport of sediment over rippled beds hinders our ability to fully understand the mechanics and effects of bedform morphology. Therefore, it is necessary to determine the correlation between three-dimensional bedform morphology, turbulence, and boundary layer shear stress to understand the complex

bottom boundary layer processes occurring over rippled seabeds. Understanding of these complex physical processes will eventually improve military operations, such as oceanographic forecasting and mine warfare, as well as have societal benefits, such as improving the design of coastal structures and prolonging the effects of coastal restoration.

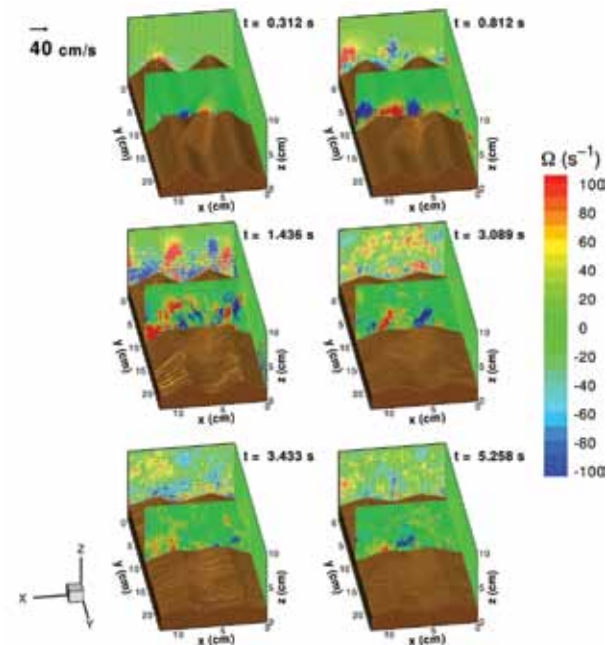


FIGURE 2 Shown are six snapshots from a bifurcated ripple simulation. The bifurcated ripple is at a 45° angle to the two parallel ripples. The flow direction is perpendicular to the ripples (in the x-direction). Contours of y-vorticity (Ω_y) are plotted in the planes bisecting the ripples (x-z planes). Contours of x-vorticity (Ω_x) are plotted in the plane parallel to the ripples (y-z plane). During the initial spin-up, the flow circulates over the bifurcation, transporting sediment into the termination areas. The bifurcation is almost completely eroded after three wave periods. Here, the boundary layer extends to the top of the simulation domain, which is more than double the boundary layer thickness over non-bifurcated ripples.

Acknowledgments: Laboratory data shown in Fig. 1 was provided courtesy of Dr. Diane Foster from the University of New Hampshire.

[Sponsored by ONR]

Reference

- ¹ A.M. Penko, D.N. Slinn, and J. Calantoni, "Model for Mixture Theory Simulation of Vortex Sand Ripple Dynamics," *Journal of Waterway, Port, Coastal, and Ocean Engineering* **137**(5), 225 (2011), doi:10.1061/(ASCE)WW.1943-5460.0000084.

High-Performance ISR Exploitation with the Geospatial Hub

E.Z. Ioup, J.T. Sample, and B.Y. Lin
Marine Geosciences Division

Introduction: Over the last several years, the military has seen an expansion in the diversity and quality of intelligence, surveillance, and reconnaissance (ISR) products available to the warfighter. Advances in remote sensing mean that raw intelligence products now include data from a diverse set of field-deployable sensors. Improvements in computing hardware allow for significantly more real-time analysis of this data. These changes require that the high volumes of data being produced by multiple diverse sensor and analysis systems be managed and disseminated in the field. NRL's Geospatial Hub (GHub) is a field-deployable Common Information Space (CIS) designed as a high-performance solution to managing these DoD sensor and intelligence products.

Data Management: The GHub CIS is the core of the GHub architecture and is designed to manage and disseminate a diverse collection of ISR products. These include imagery, vector products, Powerpoint and Word documents, sensor detections, moving object tracks, analysis products, etc. The data management

capability of the GHub CIS supports storing and indexing data products. Data is versioned to allow tracking of changes and prevent data loss. A common set of metadata is stored with the data including description, classification, geographic area, temporal extent, etc. Both the data itself and the common set of metadata are indexed to allow users to efficiently search for and discover relevant data products.

The GHub provides a Web interface to allow users to browse or search for data, both textually or geographically. They may also upload or download data products. A key feature of the GHub is its ability to customize the Web interface to the data being viewed. For example, the Web page for a collection of ISR imagery will provide previews of each image.

As an alternative to the Web interface, the GHub CISView provides a custom 3D map-based interface to the GHub CIS (see Fig. 3). It supports previewing data on a map overlaid with high-resolution DoD imagery and charts. The CISView is designed for real-time visualization of live streaming of data as it arrives in the GHub CIS. It also supports querying the GHub CIS for older data in support of forensic analysis.

Net-Centric Interfaces: The GHub supports full net-centric access to its data and services. Every core function provided by the GHub is made available through a full Web service Application Programming Interface (API). External sensor and analysis systems



FIGURE 3

The GHub CISView streaming real-time ISR data, a combination of sensors and human reporting, from the GHub CIS.

automatically download and upload data through the API, without any human involvement. By using the Web service API, ISR data may be added and retrieved from the GHub at a high rate, supporting real-time analysis and visualization operations.

The GHub also provides a suite of geospatial Web services. These services, which are standardized by the Open Geospatial Consortium (OGC), allow geospatial data stored in the GHub to be used by a wide variety of geospatial clients. Common tools such as Google Earth, ArcMap, and FalconView may all retrieve data using these services.

Synchronization: The GHub is designed to support fielded military users. To address the need for fielded users to have access to up-to-date geospatial data, the GHub includes an enterprise-level synchronization capability. A field-deployed GHub synchronizes data to a fixed-site GHub system located at a reach-back cell. The fixed-site GHub contains the master copy of all the data used by all of its connected field-deployed GHub systems. The field-deployed GHub subscribes to data on the fixed-site GHub. Whenever that data is updated, the field-deployed GHub automatically downloads it. Similarly, when data is uploaded to a field GHub, it automatically publishes to the fixed-site GHub for further distribution.

Field locations often have low bandwidth or intermittent network connections. As a result, the GHub synchronization process was designed to be resilient to these network problems. In fact, the GHub synchronization capability has been successfully tested over tactical mesh networks with intermittent connectivity, low bandwidth, and high latency. Using GHub synchronization, users never have to monitor long-distance data transfers to ensure they complete successfully; the GHub manages these automatically.

Conclusion: The GHub has served as the central data repository of the ISR architecture in a number of field exercises. The ISR architectures tested in these exercises included a large number of diverse sensor and analysis systems. By providing a standardized means of disseminating and discovering data, the GHub made it possible for these diverse systems to work together. The result was both a speedup in the ISR to Command and Control dataflow and an improvement in intelligence products available to commanders.

[Sponsored by ONR]

Underwater Applications of Compressive Sensing

G.F. Edelmann and C.F. Gaumond
Acoustics Division

Introduction: Recently, it has been shown that it is possible to exactly reconstruct a sparse signal with fewer linear measurements than would be expected from traditional sampling theory.¹ This novel and unexpected method, termed compressive sensing, is an optimization problem with a constraint that is expressed with different norms, such as l_1 or the absolute value. By solving a convex optimization problem, exact recovery of the partially sampled signal is possible. The required sampling is neither complete (e.g., Nyquist theorem) nor equally spaced. The only caveats are that the unknown signal must be sparse in some sense and we must choose the correct basis functions to represent the signal.

In this paper we demonstrate compressive sensing by applying it to a problem in underwater acoustics: the detection of a quiet ship signature, where the spectral lines are sparse in frequency space. Ship signatures are dominated by tonal lines generated by ship gearing, engine, or propeller rotation and so are candidates for compressive sensing. Despite low signal-to-noise ratio (SNR), ocean variability, and poorly sampled measurements, this technique was able to extract a ship signature in measured at-sea data. The demonstration of robustness to measured oceanic noise and to imperfect single component signal model shows that this technique has great promise for other underdetermined inversion problems in the underwater environment.

Methodology: Compressive sensing is a relatively new technique for solving inverse problems.² Inverse problems arise in several underwater acoustics applications, for example, detecting frequency lines in a time domain signal. This problem can be viewed as inverting time samples into frequency components. The typical approach using Fourier transforms implements algebraically the formalism of integral equations, treating the signals as vectors, with a distance defined in terms of root squared magnitude. This definition of a distance is similar to that of vectors in Euclidean space, where the distance is the square root of x squared plus y squared.

Compressive sensing, however, is based on the l_1 norm, which defines distance as the the sum of the absolute values of the differences of each component direction. The distance is the sum of the absolute value of x plus the absolute value of y . This mathematical approach has been used extensively in various applications, such as business and the “minimum salesman

route problem.” The l_1 norm describes the distance traveled by a taxi cab in a city with streets laid out in a rectangular grid. However, this approach is rarely used in physical sciences.

Recently, techniques using l_1 have been applied to problems closely associated with wireless communications and image compression.³ NRL is currently applying l_1 techniques to problems in underwater acoustics, such as signal detection, array processing, and array design, as well as in other areas such as radar.

Measured Ship Signature: Figure 4 shows an example of compressive sensing of at-sea data measured on an acoustic hydrophone in a towed array during the MAPEX 2000 experiment.⁴ A spectrogram of 14 seconds of typical data is shown in the top left panel of Fig. 4. The lower portion of the frequency spectrum contains chirps used for the geoacoustic experiment. After band-pass filtering, the resulting 4096 point time series is shown in the top right panel. The signal is then subsampled to just 409 points. Compressive sensing of the at-sea data is shown in the lower panels of Fig. 4. These results are remarkable. First, the technique is robust to ocean noise and variability. Second, the tone is modulated during the period, yet compressive sensing produced the center frequency. The conclusion is that the sparsity constraints successfully minimize detections in the frequency domain.

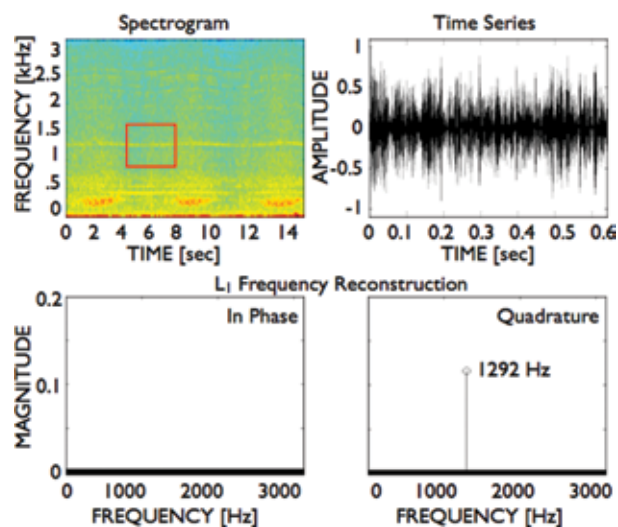


FIGURE 4 Compressive sensing of the at-sea data. The ship's signature is detected and extracted even in the presence of noise and variability.

It is difficult to produce probability of detection and false alarm rates as a function of SNR for a towed array because the ship radiation and the background noise remain fairly constant in strength. To avoid adding numerically generated white noise, the SNR was controlled by changing the size of the passband; the

effective SNR was varied from -3 to 5.5 dB. The left panels of Fig. 5 show the time series and frequency domain of the tightly band-passed modulated signal in red and the noisy bandwidth in blue. In the right panels, the probability of detection and false alarm rate are shown in the solid boxes for the at-sea data. The faint gray background lines show the numerically simulated results to guide the eye on expected performance over a larger SNR regime.

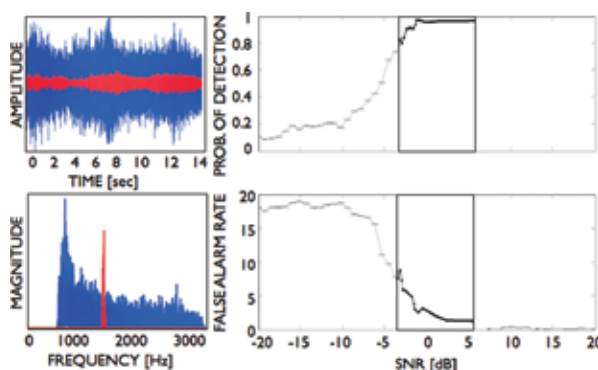


FIGURE 5 Probability of detection and false alarm rate vs signal-to-noise ratio. Even down to -3 dB SNR, the at-sea results (solid boxes) show that compressive sensing can reliably detect ship signatures.

Summary: We are adding to the U.S. expertise in anti-submarine warfare (ASW) and supporting disciplines to improve national capabilities to detect, locate, and identify targets at sea. This paper shows, for the first time, the application of compressive sensing to an ASW problem of interest. Despite low SNR, ocean variability, and poorly sampled measurements, the technique was able to extract a ship signature in measured at-sea data. The demonstration of robustness to measured oceanic noise and to imperfect single component signal model shows that this technique has great promise for other underdetermined inversion problems in undersea warfare.

[Sponsored by ONR]

References

- ¹ E. Candès, J. Romberg, and T. Tao, “Robust Uncertainty Principles: Exact Signal Reconstruction from Highly Incomplete Frequency Information,” *IEEE Trans. Inf. Theory* **52**(2), 489–509 (2006).
- ² <http://www.acm.caltech.edu/l1magic> (accessed Sept. 2010).
- ³ S. Boyd and L. Vanderberghe, *Convex Optimization* (Cambridge University Press, Cambridge, 2004).
- ⁴ M.R. Fallat, P.L. Nielsen, and M. Siderius, “The Characterization of a Range-Dependent Environment Using Towed Horizontal Array Data from the MAPEX 2000 Experiment,” SACLANCEN Report SM-402 (2002).